Research Article

Micro and nano plastics release from a single absorbable suture into simulated body fluid

Yunhong Shi [a,b], Dunzhu Li [c,*], Christopher Hill [d,e], Luming Yang [a,d], Emmet D. Sheerin [d,e], Rekha Pilliadugula [d,e], Jing Jing Wang [d,*], John Boland [d,e,**], Liwen Xiao [a,b,***]

[a] Department of Civil, Structural and Environmental Engineering, Trinity College Dublin, Dublin 2, Dublin D02PN40, Ireland
[b] TrinityHaus, Trinity College Dublin, Dublin 2, Dublin D02PN40, Ireland
[c] College of Jiyang, Zhejiang A&F University, Zhuji 311800, China
[d] AMBER Research Centre and Centre for Research on Adaptive Nanostructures and Nanodevices (CRANN), Trinity College Dublin, Dublin 2, Dublin D02PN40, Ireland
[e] School of Chemistry, Trinity College Dublin, Dublin 2, Dublin D02PN40, Ireland

HIGHLIGHTS

- Micro and nano plastics released from polyglycolic acid based absorbable sutures.
- No microplastics were released from the nonabsorbable sutures.
- Polyglycolic acid based absorbable suture underwent bulk degradation process.
- The bulk degradation process resulted in sharp-edged microplastics release.

GRAPHICAL ABSTRACT
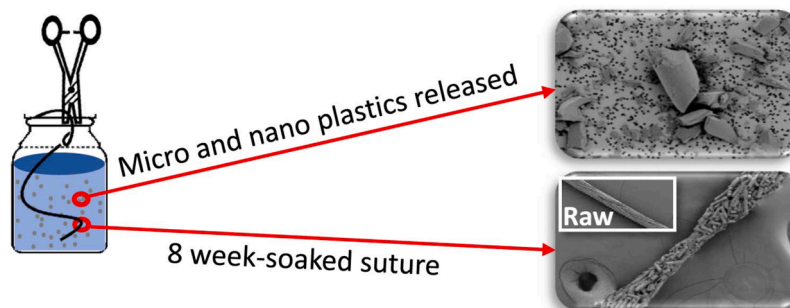
ARTICLE INFO

ABSTRACT

Synthetic polymers are widely used in medical devices and implants where biocompatibility and mechanical strength are key enablers of emerging technologies. One concern that has not been widely studied is the potential of their microplastics (MPs) release. Here we studied the levels of MP debris released following 8-week in vitro tests on three typical polyglycolic acid (PGA) based absorbable sutures (PGA 100, PGA 90 and PGA 75) and two nonabsorbable sutures (polypropylene-PP and polyamide-PA) in simulated body fluid. The MP release levels ranked from PGA 100 >> PGA 90 > PGA 75 >> PP ~ PA. A typical PGA 100 suture released 0.63 ± 0.087 million micro (MPs > 1 µm) and 1.96 ± 0.04 million nano (NPs, 200–1000 nm) plastic particles per centimeter. In contrast, no MPs were released from the nonabsorbable sutures under the same conditions. PGA that was co-blended with 10–25% L-lactide or epsilon-caprolactone resulted in a two orders of magnitude lower level of MP

---

* Corresponding authors.
** Corresponding author at: AMBER Research Centre and Centre for Research on Adaptive Nanostructures and Nanodevices (CRANN), Trinity College Dublin, Dublin 2, Dublin D02PN40, Ireland.
*** Corresponding author at: Department of Civil, Structural and Environmental Engineering, Trinity College Dublin, Dublin 2, Dublin D02PN40, Ireland.
  E-mail addresses: lidu@tcd.ie (D. Li), jjwang@tcd.ie (J.J. Wang), jboland@tcd.ie (J. Boland), liwen.xiao@tcd.ie (L. Xiao).

release. These results underscore the need to assess the release of nano- and microplastics from medical polymers while applied in the human body and to evaluate possible risks to human health.

1. Introduction

Globally, synthetic polymers have been widely used in medical implants (i.e., sutures, bone plates, joint replacement and heart valves) and devices (i.e., blood tubes, artificial hearts and biosensors), providing substantial benefits to human health [2,38,48,70]. These polymer-based medical products are generally classified into two groups based on the absorbability of the material in the body: absorbable products, such as polyglycolic acid (PGA) sutures and nonabsorbable products, such as polypropylene (PP) sutures [13,24,47]. For applications involving medical-grade polymers, it is crucial to understand the pristine properties (e.g., biocompatibility and mechanical properties) as well as any degradation processes that may lead to a loss of mechanical strength. In vitro studies using simulated body fluid (SBF) have been widely accepted as a standard tool to investigate the hydrolysis degradation and the loss of mechanical strength in medical implants, which in turn provides insights into the behaviour of the material in potential practical scenarios [5,70].

During the degradation process, these medical plastics demonstrate two modes: surface and bulk degradation, depending on the relative rate of bond cleavage and water diffusion into the bulk polymers [38,64]. These two modes generate the plastic debris (which are microplastics-MPs [20,62]) with different physiochemical properties [38]. While surface degradation results in the gradual release of MPs and nano-sized MPs (NPs) from the surface, bulk degradation often leads to the disintegration of implant to generate large debris and then high quantity of polymer particles in short term. Currently, nano- and microplastics are a global concern due to the potential risk to human and environmental health [50,62]. It was reported that MPs smaller than 10 μm can translocate from the gut cavity to the lymph and circulatory systems, causing systemic exposure and accumulation in human tissue [11,62]. Previous studies also found that the MPs with rugged or sharp morphology showed adverse effects on cell membrane [8,12]. Though the specific risk is still unknown, previous reported high levels of MP exposure are an early warning of potential human health risks. Notably, extensive in vitro testing of sutures has been conducted over the past 50 years [17,18,59], focussing primarily on mechanical and chemical properties [2,24]. However, to the best of our knowledge, there is no study systematically investigating the release level, speed, morphology and detailed release mechanism of MPs during the degradation of implanted medical plastic products such as sutures. This information is crucial given the potential direct relation to human health.

To fill this critical gap, this study aims to systematically characterize the release of MPs from typical sutures and provide insights into the release mechanism. Three PGA-based absorbable sutures and two nonabsorbable sutures were soaked in SBF for 8 weeks following the standard ASTM F1635 protocol. The released particles in SBF were captured and investigated using Raman spectroscopy and scanning electron microscopy (SEM). As to the nano-sized MPs (NPs), the release number/mass and chemical identity was confirmed using SEM and total organic carbon (TOC) analyzer. An in situ test was also conducted for 8 weeks to understand the suture degradation mechanism and MPs release process.

2. Materials and methods

2.1. Methods to prevent sample contamination

Throughout the experiment, thoroughly cleaned boro 3.3 glassware were used for sample preparation. Deionized (DI) water (resistivity of 18.2 MΩ. cm) was used for all cleaning procedures. Particle-free nitrile

gloves, cotton-based laboratory coats and lab caps were worn all the times. Blank samples (DI water) and control samples (SBF without suture) were used to ensure the contamination elimination and the reliability of the testing protocol [39]. Silicon (Si) and germanium (Ge) wafer substrates were washed with HPLC grade ethanol before use.

2.2. Preparation of SBF

SBF suggested by standard protocol (e.g., ASTM F1635) is a solution with ion concentrations equal to that of human blood plasma and is typically buffered to physiological conditions [26,36,4,61,73]. Hence, SBF was used in this study. It was prepared by dissolving quantities of sodium chloride (NaCl, Merck), sodium bicarbonate (NaHCO$_3$, Corning), potassium chloride (KCl, VWR Chemicals), potassium hydrogen phosphate trihydrate (K$_2$HPO$_4$3 H$_2$O, Sigma-Aldrich), magnesium chloride (MgCl$_2$6 H$_2$O, Merck), calcium dichloride (CaCl$_2$, Sigma-Aldrich), sodium sulfate (Na$_2$SO$_4$, Sigma-Aldrich) in DI water [61]. 1 M HCl was used to adjust the pH of the SBF to 7.4. The specific ion concentrations of SBF solution are listed in Table S1.

2.3. Long-term study of the suture degradation process

Following the established standard (ASTM F1635), released MPs and the suture degradation process were tested. Three types of absorbable sutures and two types of nonabsorbable sutures were chosen for long-term study. The absorbable sutures were PGA, polyglactin 910 (Vicryl), and poliglecaprone 25 (Monocryl) and the non-absorbable sutures were PP and polyamide (PA). In this study, PGA, polyglactin 910 (Vicryl), and poliglecaprone 25 (Monocryl) were designated as PGA 100, PGA 90 and PGA 75 based on the glycolic acid content in the suture. Detailed information of five types of sutures used in this study is presented in Table 1.

Glass rods were cleaned thoroughly and dried and the sutures were then loosely wrapped around the glass rod with a total suture length of around 300 cm. All suture used in this study were size of 5–0 with a diameter of 150 nm. The sutures attached to glass rods were soaked in 100 mL SBF solution in glass bottles. The glass bottles were placed in the thermal shaking bath with a fixed water temperature of 37 ℃ and shaking speed of 100 rpm/min, similar to a previous study [25]. Only the glass rod was soaked in 100 mL SBF solution for the control sample. These long-term studies were conducted for 8 weeks.

In situ testing was performed to examine the suture at different stages in the degradation process. The PGA 100 suture involved fixing the pristine suture onto a precleaned stainless-steel mesh that was soaked in the SBF in a glass bottle. Then the glass bottle was placed in the thermal shaking bath with the same water temperature and shaking speed as described above. Changes in the suture morphology at the same location on this PGA 100 suture was recorded with SEM on week 0, week 2, week 4 and week 8.

2.4. Identification and quantification of MPs and NPs

To quantify the number of MPs released, samples were taken from the well mixed and carefully shaken SBF solution in week 8. To minimise the impact of background particles from the SBF, all the samples were treated with 1 M HCl for 24 h at room temperature before filtration, following a previous study [9]. After HCl treatment, the samples were gently shaken and filtered through the gold-coated polycarbonate (PC) membrane filter (APC, Germany Ltd) with a pore size of 0.8 μm for Raman, followed by SEM analysis, as detailed in Fig. 1a. Raman spectra were obtained over the range 250–3200 cm^{-1}. In this study, Raman

Table 1
Detailed information on five types sutures used in this study.

|	Absorbable suture			Nonabsorbable suture	
Name in this study	PGA 100	PGA 90	PGA 75	PP	PA
Suture types	Polyglycolic acid	Polyglactin 910 (Vicryl)	Poliglecaprone 25 (Monocryl)	Polypropylene	Polyamide 6 or Polyamide 6,6
Polymer types	Homopolymer	Copolymer	Copolymer	Homopolymer	Homopolymer
Composed of	100% glycolide	90% glycolide and 10% L-lactide)	75% glycolide and 25% epsilon-caprolactone	Polypropylene	Polyamide
Molecular Formula	$(C_2H_2O_2)_n$	$(C_2H_2O_2)_m(C_3H_4O_2)_n$	$(C_2H_2O_2)_m(C_6H_{10}O_2)_n$	$(C_3H_6)n$	$(C_6H_{11}NO)n$ or $(C_{12}H_{22}N_2O_2)n$
Coating material	Calcium stearate Polycaprolactone (PCL)	Calcium stearate, 70% L-lactide and 30% glycolide	No	No	No
Filament structure	Multifilament	Multifilament	Monofilament	Monofilament	Monofilament
Hydrolyzate	Glycolic acid $(C_2H_4O_3)$	Glycolic acid $(C_2H_4O_3)$ Lactic acids $(C_3H_6O_3)$	Adipic acid $C_6H_{10}O_4$	N/A	N/A
Fully absorbed time	Approximately 42 days	56 - 70 days	91–119 days	N/A	N/A

N/A-not available
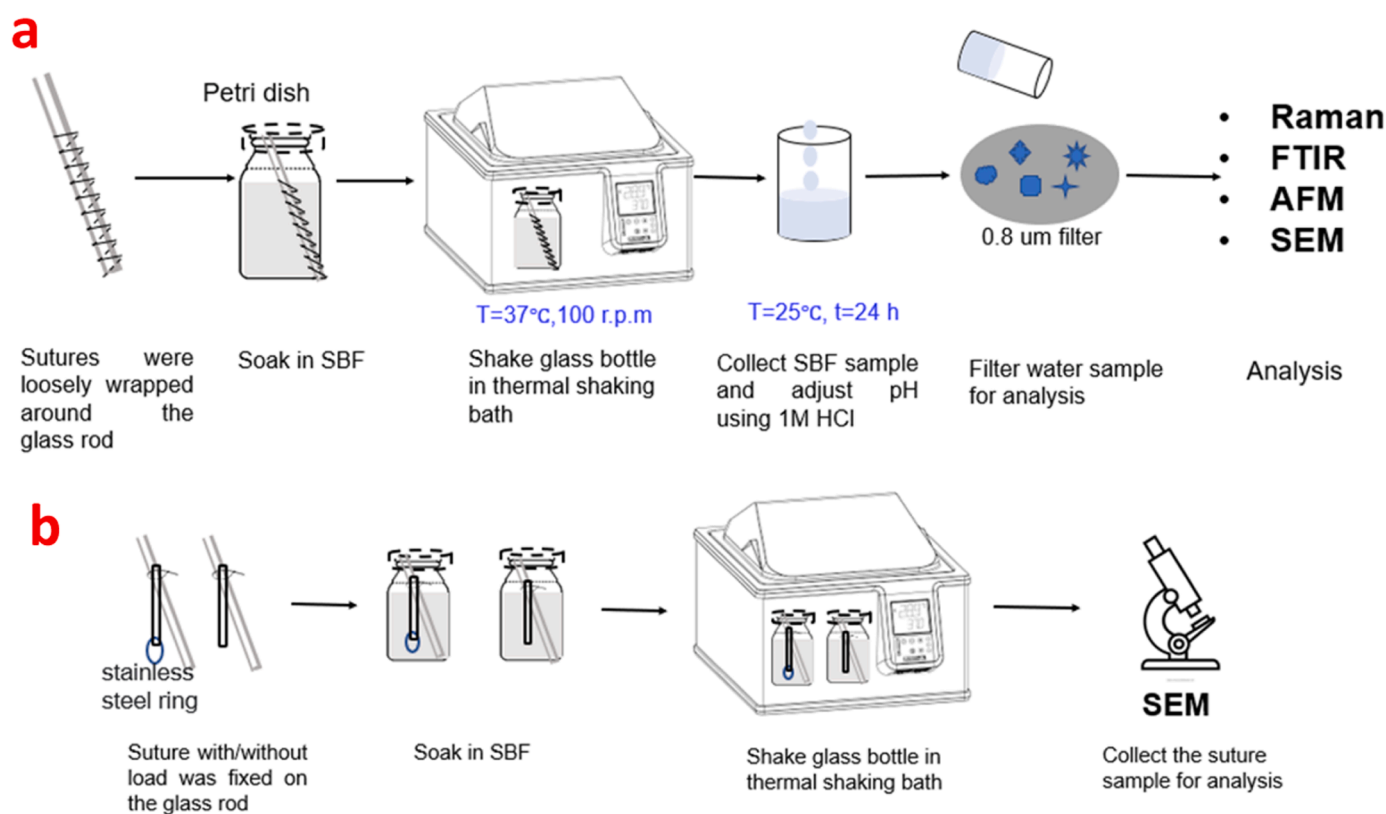
Fig. 1. (a) Schematic of suture sample preparation; (b) Schematic showing the degradation process of suture under load.

peaks in the ranges of 900–1800, 2900–3000 cm^{-1} were used to determine the chemical composition of PGA-MPs. Referring to previous reports [33,52,53,69], the hit quality index (HQI) of 0.7 was chosen as the threshold value to confirm whether the detected particle is PGA-MPs. Renishaw InVia Raman spectrometer was used to identify the MPs released from suture and the test size limitation was 1 μm. A silicon wafer was used to calibrate the Raman system by checking the peak location (520 cm^{-1}) and peak intensity (>6000 counts) before each test. ImageJ software was used for quantification and determining the size of MPs.

To identify and quantify the nano-sized MPs (NPs, <1000 nm) released from PGA 100, the HCl treated samples following week 8 were passed through a membrane filter with a pore size of 1 μm (Whatman, UK) to remove the large particles and the filtrate was collected. Then the filtrate was passed through a gold-coated PC membrane filter (APC, Germany Ltd) with a pore size of 0.2 μm for SEM analysis. The particles on the membrane filter (0.2 μm) were also washed and resuspended using DI water, then drop casted and dried onto the Ge wafer for SEM imaging. To obtain the mass distribution of different size range of nano particles, the HCl treated samples following week 8 was sequentially filtered by the membrane filters with pore sizes of 1 μm (Whatman, UK), 0.8 μm (APC Ltd), 0.45 μm (Whatman, UK), 0.2 μm (APC Ltd) and 0.05 μm (Whatman, UK). The TOC concentration of the filtrate from each step was tested and the TOC for NPs distribution was calculated by the difference between the filtrate. The diameter of all membrane filters was 25 mm.
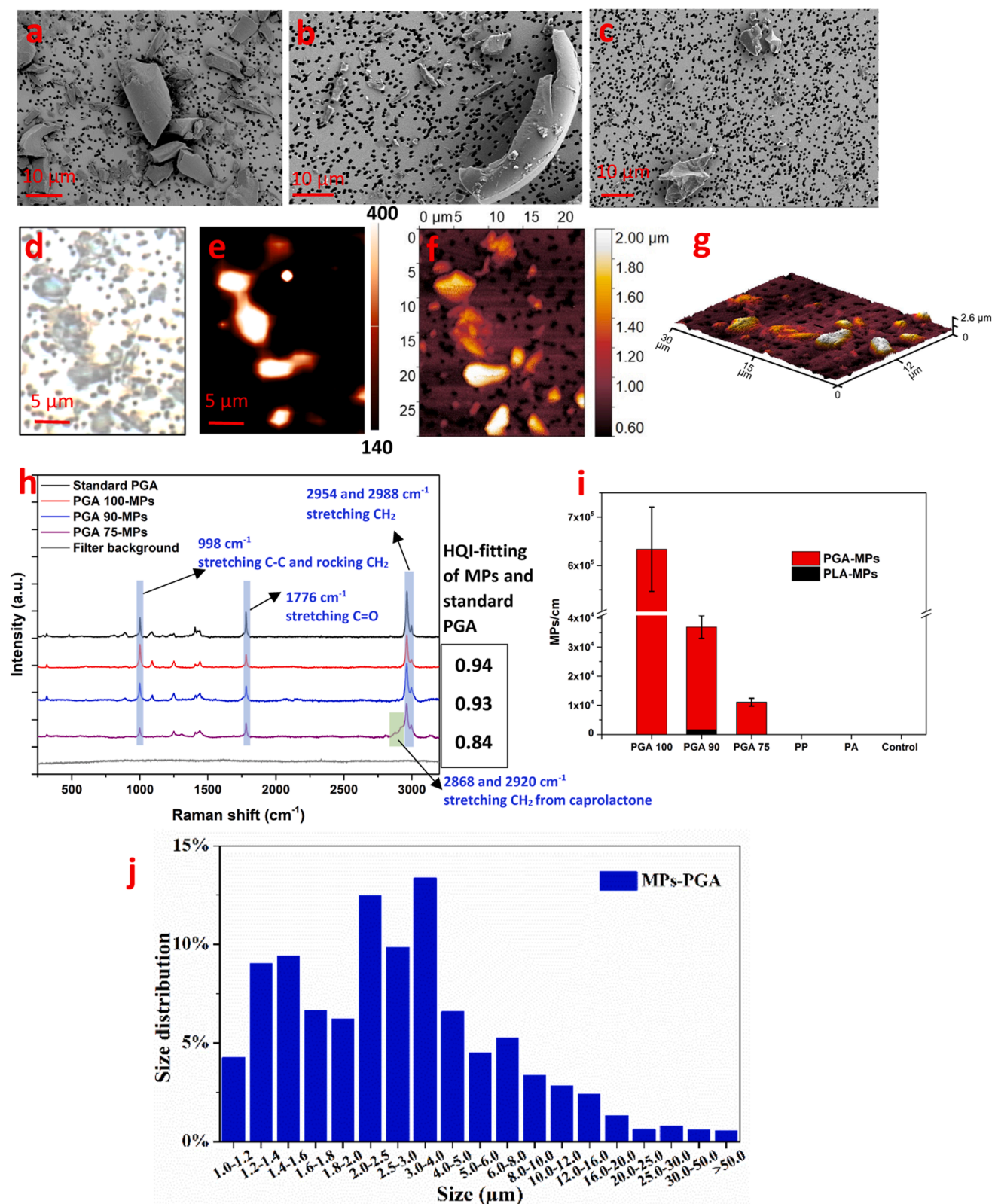
Fig. 2. SEM images of MPs captured from 8 weeks soaked SBF sample of PGA 100 (a), PGA 90 (b) and PGA 75 (c), respectively; (d-g) Identification and mapping of typical PGA-MPs. d, Optical microscope image of particles released from PGA 100 suture using a 100 × microscope objective. e, Raman mapping of the same region obtained using the PGA Raman bands at 2940–2980 cm^{-1}. The colour scale bar indicates the intensity of the integrated spectral band in arbitrary units. (f) AFM image of the same region to determine the morphology of released MPs. The colour scale bar indicates the height of MPs. (g) Three-dimensional (3D) AFM topographic image. (h) Raman spectra of standard PGA polymer, typical PGA-MPs from PGA 100, PGA 90 and PGA 75 sample, and filter background, respectively; (i) The number of MPs release from a single centimeter of suture after soaked in SBF for 8 weeks. (j) The size distribution of PGA-MPs (8 weeks soaked PGA 100 sample).

2.5. The degradation process of suture under mechanical load

Given that external force may be applied during suture use, the degradation process of PGA 100 under tension was performed for 4 weeks to check whether it had a significant impact (Fig. 1b). Glass rods and stainless-steel ring were cleaned thoroughly and dried. The sutures were then fixed on the glass rod at one end while a stainless-steel ring was affixed to the other end. The weight of the stainless-steel ring was 0.1 Newtons similar to the force applied to a suture used on wound [6]. After that, the tied stainless-steel ring was vertically hung during the experiment, see Fig. 1b. The sutures under tensile load were soaked in 100 mL SBF solution in glass bottles. The glass bottles were placed in the thermal shaking bath as described in 2.3. For the control sample, PGA 100 without load was soaked in 100 mL SBF solution.

2.6. Characterization of the suture degradation process

SEM-EDX (Zeiss Ultra Plus) with an acceleration voltage of 15 kV was performed to characterize changes in the suture structure during the degradation process. The morphology of released MPs was acquired by atomic force microscopy (AFM, NT-MDT) with a tapping mode probe (Nanosensors, PPP-NCST). Gwyddion 2.54 software was used to analyse AFM results. TOC analyser (Shimadzu, TOC-L) was used to test the TOC concentration.

3. Results

3.1. Microplastics release from sutures

Micro-sized particles released from five types of sutures into SBF (after 8 weeks) were captured and tested following the method of Fig. 1a. SEM images of MPs captured following 8 weeks of exposure to SBF solution for PGA 100, PGA 90 and PGA 75 suture are shown in Fig. 2a-c. As presented in Fig. 2a and b, rod-like MPs with diameters of around 10 μm were found, which may be due to the breakdown of the filamentary structure of PGA 100 and PGA 90. Only irregular fragments were found in the case of PGA 75. No MPs were detected from the control, the PP or the PA samples during the study period (Fig. S1). This

indicates that no significant degradation of PP and PA sutures after soaking in the SBF for 8 weeks.

Raman spectroscopy confirmed that the majority of captured particles from all absorbable sutures had spectra that matched the standard PGA spectrum (standard PGA polymer was purchased from Sigma-Aldrich) [7,34], indicating that they were PGA MPs (Fig. 2h). Raman spectra also confirmed that these MPs were polymeric, rather than monomers or oligomers. The primary difference between monomer/oligomer and polymeric glycolic acid is that the polymer has double peaks at around 1425–1427 cm^{-1}, due to the presence of ester groups ([-CH$_2$-COO-]$_n$) within the repeating unit of poly(glycolic acid) [7]. In addition, Raman tests confirmed that most of the MPs had high crystallinity as detailed and described in SI. Similarity analysis found that the overall HQI of PGA 75-MPs compared to standard PGA was around 0.84, which was lower than that of PGA 100-MPs (around 0.94) and PGA 90-MPs (around 0.93). The Raman spectra of PGA 75-MPs had clear peaks at 2868 and 2920 cm^{-1} which were associated with the stretching of CH$_2$ from the caprolactone units (Fig. 2h and S2).

The number of MPs released is shown in Fig. 2i. PGA 100 released 0.63 ± 0.087 million PGA-MPs per centimeter suture length after 8-weeks. Most of these MPs were smaller than 5 μm with sharp edges. PGA 90 and PGA 75 released substantially lower levels of MPs; 0.037 ± 0.0041 million/cm and 0.011 ± 0.0013 million/cm, respectively and only 5.9% and 1.7% of that released from PGA 100. Evidently, copolymerization with other materials can substantially reduce the level of MP release given the much lower MP quantity obtained from PGA 75 and PGA 90 when comparing to that of PGA 100. In terms of MPs type, only PGA-MPs were identified from PGA 100 and PGA 75. Interestingly, for PGA 90 there were 1592 ± 175/cm polylactic acid (PLA) MPs detected in the solution, which accounted for 4.3% of the total MPs.

3.2. Nano-sized microplastics release from PGA 100 suture

To investigate NP release, 10 mL of the 8-week SBF solution exposed to PGA 100 was filtered through membrane filters with a pore size of 1 μm first. To avoid aggregation (Fig. 3a) and accurately quantify particles numbers and sizes, NPs in the filtrate with size ranges from 200–1000 nm were captured using an Au-coated PC membrane filter
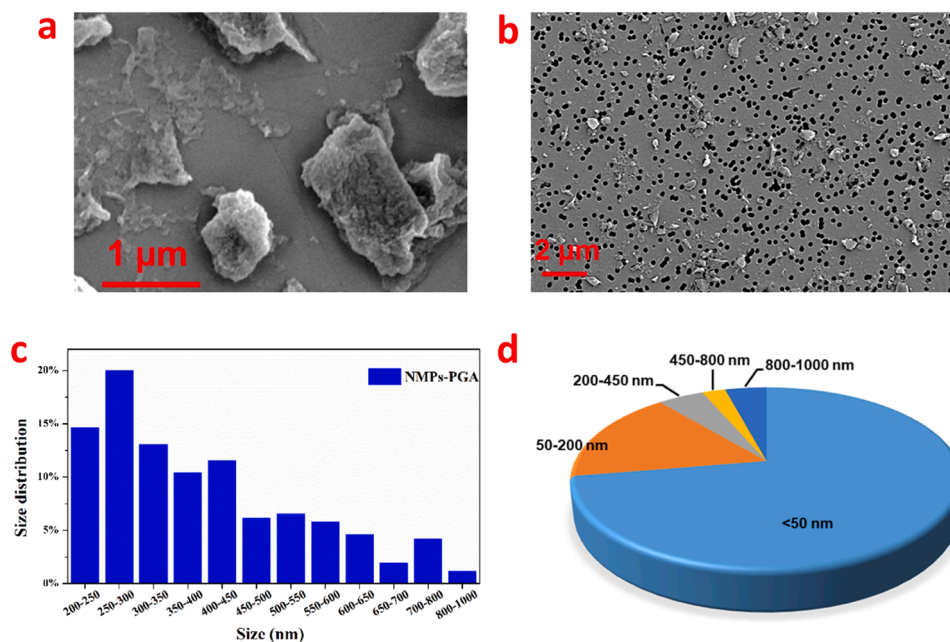

Fig. 3. (a) PGA 100 released nano particles (200–1000 nm) drop casted on a Ge wafer. (b) SEM image of PGA 100 released nano particles (200–1000 nm) captured by filter with pore size of 200 nm. (c) The size distribution of nano particles captured by the filter with pore size of 200 nm. (d) The TOC percentages from different size ranges of nano particles release from PGA 100 suture.

with a pore size of 200 nm and then imaged using SEM. The 200–1000 nm NPs are easily distinguished against the membrane background (Fig. 3b), and SEM analysis showed that around 1.96 ± 0.04 million NPTs (200–1000 nm) are released per centimeter of PGA 100 suture, with 70% of the particles in the size range from 200–500 nm (Fig. 3c). Particles captured on membrane filters (0.2–1 μm) were also re-suspend using DI water and carefully drop cast and dried onto a Ge wafer (Method 2.4). SEM found that the coarse surfaces of these nano particles on the Ge wafer (Fig. 3a) are consistent with the topography of the several micron-sized MPs confirmed by Raman spectrum (Fig. 2a).

Though the chemical composition still needs to be confirmed, a high proportion of these nano particles are likely nano-sized PGA.

A separate analysis of the distribution of NPs (<1000 nm) was undertaken using organic carbon mass (mg C, tested by a TOC analyser similar to a previous study [31]) to overcome the particular difficulty of accurately detecting NPs smaller than 200 nm (Fig. 3d). The sample was sequentially filtered through the membrane filters with pore sizes of 1 μm, 0.8 μm, 0.45 μm, 0.2 μm and 0.05 μm (details see method 2.4). Surprisingly, the mass distribution is dominated by NPs smaller than 50 nm (72.4%) while the NPs in the range of 800–1000 nm,
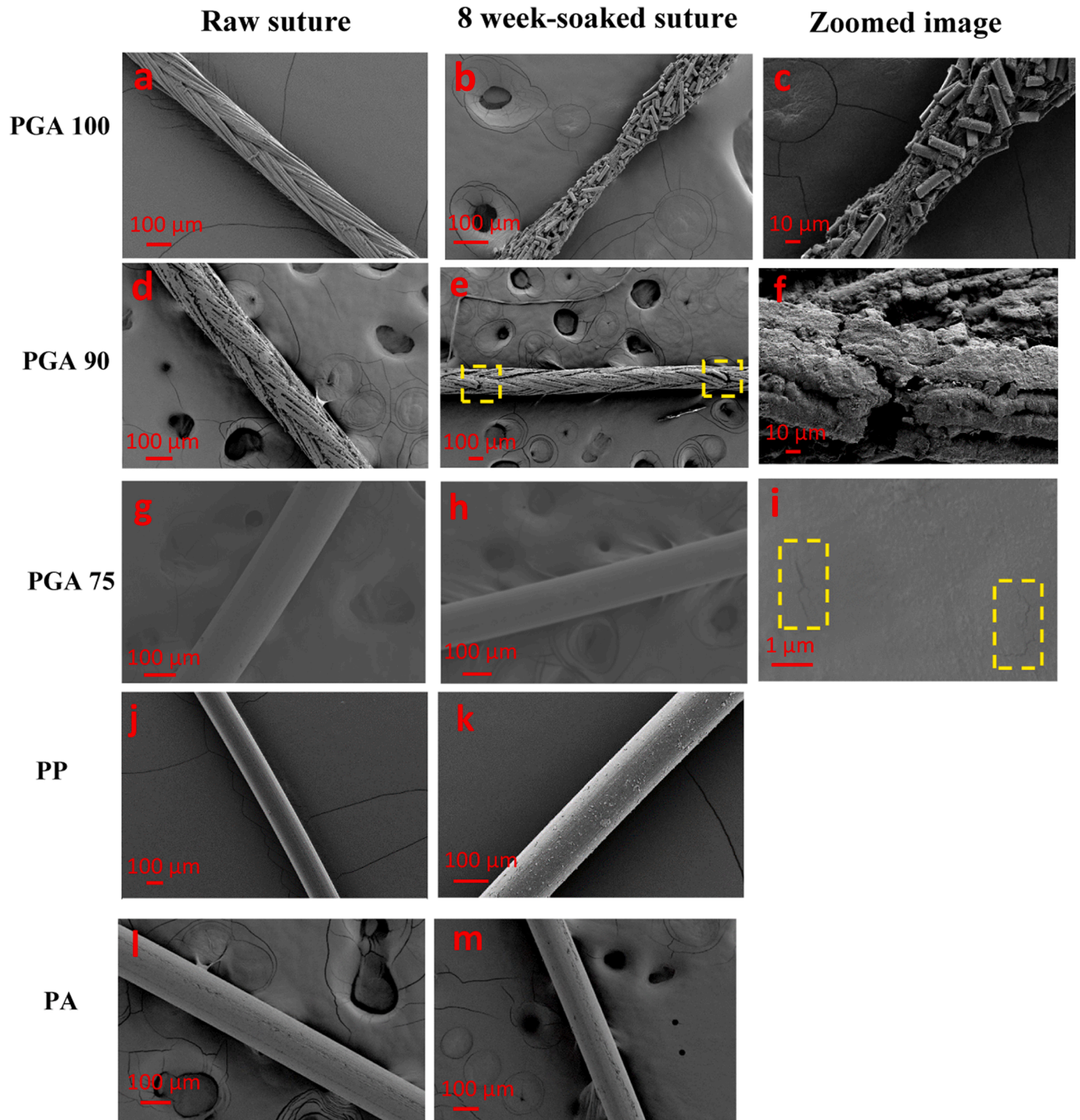

Fig. 4. SEM images of Raw PGA 100 (a), PGA 90 (d), PGA 75 (g), PP (j) and PA (l) suture; After 8 weeks soaking in SBF PGA 100 (b and c), PGA 90 (e and f), PGA 75 (h and i), PP (k) and PA (m) suture.

450–800 nm, 200–450 nm and 50–200 nm account for 4.1%, 2.3%, 4.6% and 16.6% of the TOC, respectively. It can be suspected that the large number of NPs smaller than 50 nm may be generated either by the initial degradation of the suture filaments or via a secondary processing involving larger MPs and NPs (50–1000 nm). It was reported that the high levels of secondary nanoplastics can be produced from a biodegradable microplastics under typical environmental conditions [22]. Either way, conducting particle-based analysis of these NPs will be necessary to confirm their chemical state (polymer, monomer, oligomer or other organic by-product during the degradation), which is critical for any risk assessment.

3.3. Morphological changes following exposure to SBF

Changes in the surface morphology of the bulk sutures are consistent with the release of MPs in SBF. The raw PGA 100 suture was a braid comprised of multiple PGA filaments with the coating material of polycaprolactone and calcium stearate. The average diameters of the PGA 100 suture and a single filament were around 150 μm and 10 μm, respectively. Compared with pristine PGA 100 suture (Fig. 4a), after 8 weeks all PGA 100 filaments were seen to break into rod-like segments with lengths around 10 to 100 μm (Fig. 4b). These broken rods had diameters of around 10 μm, which perfectly matched the size of some big
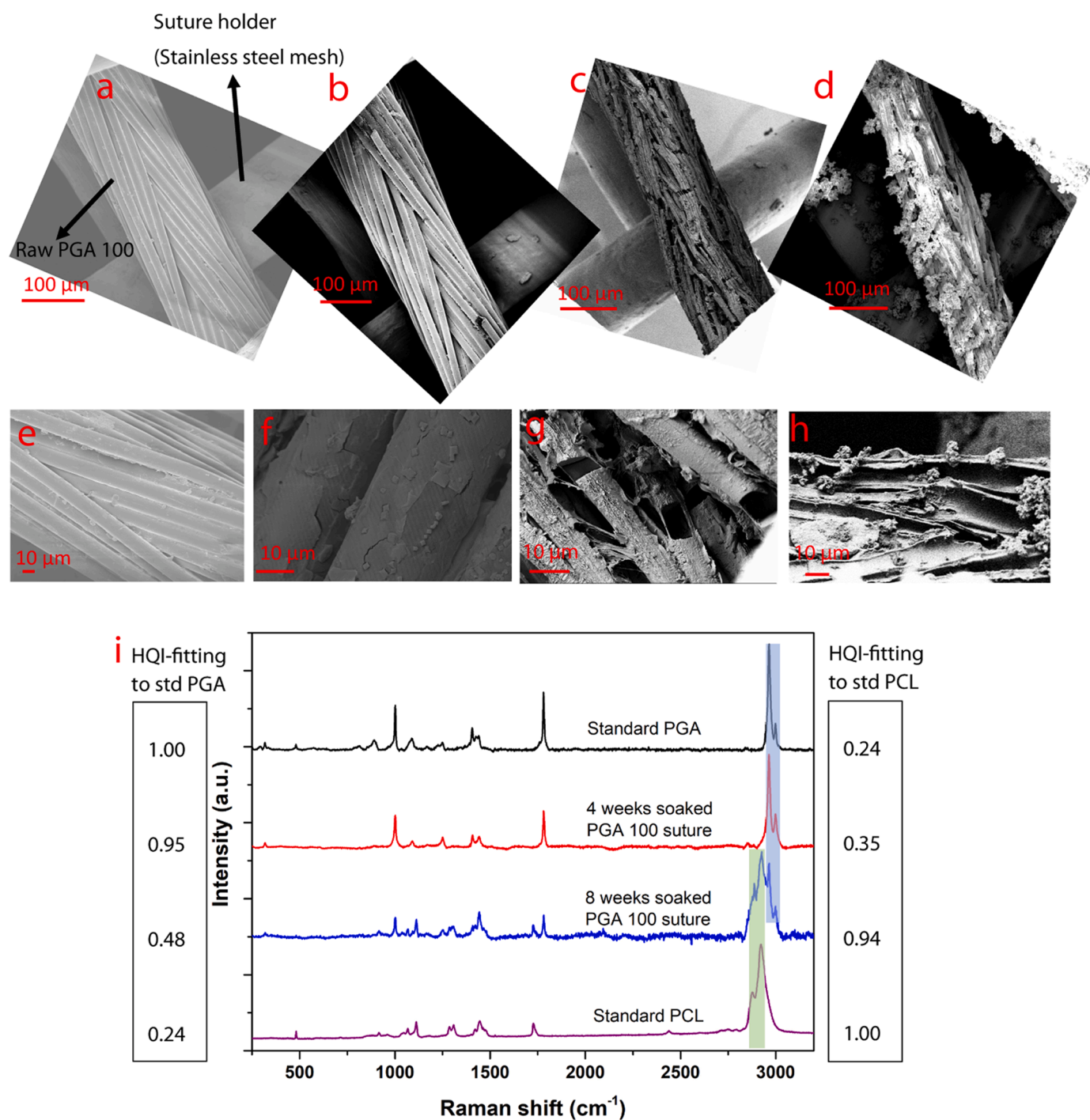
Fig. 5. In situ test of PGA 100 suture. SEM images of raw PGA 100 suture (a) zoomed image I; soaked in the SBF for 2 weeks (b and f); 4 weeks (c and g) and 8 weeks (d and h). (i) Typical Raman spectrum of standard PGA polymer, 4 weeks soaked PGA suture, 8 weeks soaked PGA suture and standard PCL polymer.

PGA MPs captured from SBF (Fig. 2a), suggesting these rods directly detach from the bulk suture. It is also noticeable that the degradation process along the length of the suture sample was not uniform. After 8 weeks, some parts of the suture were full of small rods with widths similar to that of the pristine suture. In comparison, some parts of the suture had only coating debris with a few small broken rods, while its width was only half of the raw suture. After 8 weeks of soaking, all filaments in PGA 100 turned into rod-like segments. In comparison to original well-braided filaments, the diameter of these rod-like segments kept stable, with around 10 μm. Additionally, all these segments showed a smooth surface without coarse morphology or observable surface erosion, indicating that these segments likely experienced a bulk disintegration rather than a surface degradation [38].

PGA 90 and PGA 75 showed substantially different levels of surface degradation after 8 weeks of exposure to SBF. Significant cracks were observed on the surface of PGA 90 (yellow boxes in Fig. 4e), while some micron-sized cracks appeared on the surface of PGA 75 (yellow boxes in Fig. 4i). Evidently, the degradation levels of the PGA copolymer were much slower than that of PGA 100 under the same conditions, consistent with MP release levels. It was reported that the degradation rates of absorbable materials can be tailored by copolymerising and/ or blending materials with different degradation rates [38,70]. In comparison, pure PGA has a rapid degradation rate, PLA has a medium rate, while PCL exhibits a relatively slow degradation rate [44,70]. Adding epsilon-caprolactone and L-lactide clearly slowed down the degradation rate of PGA-based sutures in this study. Additionally, the copolymer ratio may also influence the degradation level. The morphology variations clearly proved the change of degradation speed. PGA 100 with 100% of glycolide completely broken into rod-like segments, PGA 90 with 90% of glycolide only generated several cracks, while the cracks on the surface of PGA 75 with lowest glycolide composition (75%) were rare. Additionally, the released MPs captured from PGA 90 and PGA 75 only respectively account for 5.9% and 1.7% of that released from PGA 100, which is also consistent with the degradation rate change.

In contrast, nonabsorbable sutures of PP and PA, comprised of a single PP and PA filament with a diameter of around 100 μm, showed no change after soaking in the SBF for 8 weeks (Fig. 4k and m) except for a small number of white particles attached on the surface, most likely salt deposition from SBF. After further increasing the soaking time to 20 weeks there was still no evidence of degradation or cracking on the PP and PA suture surface, and no MPs were released into the SBF (Fig. S3). These results are consistent with their highly recalcitrant nature and poor biodegradability reported in previous PP and PA studies [39,44].

3.4. In situ test for the degradation process of PGA 100 suture

In-situ tests were conducted to study the PGA 100 suture degradation process by fixing the raw PGA 100 suture onto a stainless-steel mesh sample holder soaked in SBF for up to 8 weeks (Fig. 5). Compared with raw PGA 100 suture (Fig. 5a), significant separation between PGA 100 filaments and the surface coatings was observed after 2 weeks (Fig. 5b and f). Random fissures appeared on the surface coatings, which enhanced the contact between SBF and PGA filament inside. Cracks of filaments were rare, and the suture largely maintained its original shape. However, after 4 weeks (Fig. 5c and g), many crosscut cracks appeared on the suture and cracked rod segments began to appear. These cracked rod segments maintained the same diameter as the filaments of the raw suture, with lengths from 50 to 200 μm and were often connected by the coating material, which caused the majority of PGA rods to remain connected to the bulk suture. After 8 weeks (Fig. 5d and h), most of the rod like PGA segments had detached from the coating material, and only the remnants of the coating materials were observable (Fig. 5h, hollow semi-cylinders). Raman spectra confirmed that after soaking in the SBF for 4 weeks, a clear PGA spectrum can still be obtained from the bulk suture, with a HQI compared to standard PGA of 0.95. However, after 8 weeks, the Raman spectrum of the bulk suture changed, and only the

PCL coating material was observed with a HQI of 0.94. The Raman peak at 2920 cm^{-1} associated with the stretching of CH$_2$ within the repeat unit of PCL is clearly observed [37,66].

4. Discussion

This paper specifically investigated the hydrolysis of typical sutures and confirmed that the MPs release rate for the studied samples is PGA 100 $>>$ PGA 90 $>$ PGA 75 $>>$ PP = PA. The degradation and MPs release of sutures are consistent with changes in the physical and absorption properties. PGA 100 suture has the quickest strength reduction speed among these sutures and could be absorbed in around 40 days. In comparison, PGA 75 requires around 120 days to fully absorb (Table1, data from manufacturers). Compared with PGA 100-MPs and PGA 90-MPs, the HQI of PGA 75-MPs was lower and this is likely due to PGA 75 suture containing 25% epsilon-caprolactone units copolymerized with glycolic acid units. For instance, epsilon-caprolactone units can generate extra peaks at 2868 and 2920 cm^{-1} due to the well-known stretching of CH$_2$ [66]. Regarding PGA 90, PLA MPs released from PGA 90 suture and the use of PLA-based coating material [41,71] in PGA 90 is likely the source of those PLA MPs. The degradation of PGA 100 suture is a typical bulk degradation process in which the speed of water diffusion into polymer bulk is much faster than the degradation rate of the polymer backbone [64]. The bulk degradation process leads to the bulk cracking and disintegration rather than surface erosion. This can be evidenced by the smooth surface of captured PGA 100 rods on the membrane filter (Fig. 2a). Surface degradation only occurred to polymer of PGA, when the size was larger than the threshold value of 7.4 cm [64]. For PGA 100 bulk suture, the size of degraded bulk suture and released MPs can never be larger than that of the raw PGA filament. Hence, PGA 100 suture and PGA 100 MPs will undergo bulk degradation during their lifecycle in hydrolysis conditions. Unlike surface degradation, bulk degradation can lead to a sudden disintegration generating debris with random sharp edges, which may enhance the potential risk to contacted cells and organisms [8].

The number of microplastics (MPs $>$ 1 μm) and nano plastics (NPs, 200–1000 nm) released from atypical PGA 100 suture was 0.63 ± 0.087 million and 1.96 ± 0.04 million per centimeter, respectively. The quantity of MPs and NPs released per gram of bulk materials in this study is higher than in previous reports [21,28,29,40,54], which is primarily due to the bulk degradation process disintegrating almost all sections of bulk suture into MPs (Fig. 5). MPs release rates were substantially reduced when PGA monomers copolymerise with L-lactide and epsilon-caprolactone monomers. By introducing 25% of epsilon-caprolactone monomers, the MPs release rate can be decreased by two orders of magnitude (Fig. 2i). It was also reported that the degradation speed of absorbable materials could be modified by changing the polymer crystallinity, molecular weight and hydrophobicity, which will certainly change the MPs release rate [19,60,65]. Additionally, in this study, the degradation process of PGA 100 suture with the force of 0.1 N was also investigated to check the influence of tension. The force applied here was similar to the previous report [6]. There was no significant difference in the degradation process of PGA 100 sutures with and without load (Fig. S4). Although 0.1 N force has insignificant impact on MP release, further investigation is required given that the sutures used at joint wounds may experience much higher forces.

Although there were no MPs release detected from nonabsorbable sutures of PP and PA in the mild experimental conditions reported here (shaking: 100 rpm/min, pH: 7.4), the potential release of MPs is expectable under harsh service conditions. High levels of MPs release due to mechanical forces alone or combined with other factors (i.e., UV exposure) was confirmed in ocean [56] and freshwater [15] environments, as well as daily use plastic products [67]. Polymers used inside of the human body may experience high load/stress [3,48]. More importantly, the stress cycles associated with joint motion can reach as high as

1 million cycles annually [48]. A previous study on Polyethylene (PE)-based knee prosthesis showed that after 1 year of use, the total number of released particles in synovial fluid reached 9–116 million with sizes of 0.67–0.78 μm due to wear of the medical polymer [45]. The pressure exerted on the human hip joint can reach up to 18 MPa when transitioning from a sitting to a standing position [30]. In general, this value was much higher than that of plastic subjected in environmental conditions. For instance, the pressure of water scouring and wind blowing on the surface of a PP plastic film typically was around 1000 Pa and 70–850 Pa, respectively [10]. However, this value in deep ocean could substantially increase to up to 100 MPa with the increase of water pressure [72]. The release of MPs from both absorbable and nonabsorbable sutures might also be influenced by other factors, such as the locations the sutures are used and the body fluid salt concentrations and enzymes [38,57]. Salt in the fluid may form a passivation film to cover the surface of sutures, which could delay the release of MPs [55]. It also should be noted that this suture test was conducted in the simulated body fluid to investigate degradation via hydrolysis. It is different from the real human body fluid which contains different types of proteins, cells and chemicals. Simulated body fluid can be modified by spiking different types of proteins, macrophages and chemicals to well mimic the potential influence of such as protein adsorption on the surface of bulk plastic and the following change of MPs release from sutures. Future in vivo studies are also required to further validate and extend these findings [38].

Both absorbable and nonabsorbable medical polymers have their unique advantages. Using absorbable medical polymers eliminates the follow-up visits to remove the polymers from human bodies, which could decrease scarring and the chances of infection and save health care resources [42]. In contrast, nonabsorbable polymers can retain their tensile strength after long-term implantation and have low tissue reactivity [13,24]. These plastic materials are widely used in not only sutures [46], but also bone plates, joint replacement, heart valves, vascular scaffolds etc [2,27,46,48].

A previous study pointed out that PGA plastic components with sizes smaller than 7.4 cm will undergo bulk degradation with a sudden disintegration and the potential release of particles larger than 5 mm [64]. Currently, only plastic particles smaller than 5 mm are considered as MPs, which is primarily derived from the view of ocean plastic pollution [20]. Evidently, uncontrollable particles release larger than 5 mm should also be investigated for medical plastics, and the size range of MPs should be redefined based on the plastic application scenarios.

To date, there is still no consensus on the specific risk of these MPs. While in vitro toxicity tests using bioluminescent bacteria showed that after soaking PGA and PLA in SBF for 10 days and 4 weeks, respectively, both solutions became toxic [58]. The toxicity was believed to be due to the degradation products of glycolic acid and lactic acid [58], while the importance of MP as a degradation product had not been recognized at that time. During the use of PGA and PLA material, chronic inflammation (such as macrophages and giant cells) was observed [1,35]. Previous studies also found that particles that have broken-off from PLA (either by pre-degraded PLA implantation or PLA particles injection) were covered by macrophages and giant cells, which was a sign of inflammation [51,63]. However, other researchers argued that these particles were just phagocytosed by macrophage and multinucleated giant cells, so they had no adverse biological toxicity [1,14]. There is still a huge gap to fully understand the specific risk posed by those absorbable MPs. Future studies should include cell experiments, particularly with macrophages to comprehensively and accurately assess the toxicity, blood compatibility and cytocompatibility of these released MPs. Macrophages present in all human body compartments (e. g., digestive system). It is especially true that macrophages play a central role within the innate immune response to foreign particulate matter, such as microplastics [23]. Macrophages experiment has been employed to assess the toxicity of non-absorbable MPs. For instance, evaluation using fragment-type PP and polystyrene (PS) particles found that

weathered MPs showed less significant toxicity to THP-1 macrophages due the reduced level of the reactive oxygen species [32]. Similarly, a study involving PS and Polymethyl methacrylate (PMMA) also reported that human macrophages derived from isolated monocytes were highly sensitive to pristine MPs, dependent on MPs polymers and size [68]. Surface morphology also affects MPs' toxicity. A previous study focusing on macrophage internalization found that environmentally-exposed, non-absorbable PS MPs were internalized significantly more than that of pristine PS MPs due to the formation of eco-corona on the surface of MPs after environmental exposure [49]. It was also reported that the phagocytosis of PS MP by macrophages induced a metabolic shift toward glycolysis and a reduction in mitochondrial respiration and cytokine gene expression associated with glycolysis [43].

To date, the relevant cell studies focusing on absorbable MPs is rare. In future research, it is important to note that the exposure pathway of implanted medical plastics differs from that of oral/lung pathways studies previously. Additionally, these absorbable plastics can simultaneously release microplastics, additives, oligomer and monomer (glycolic acid in this study). A previous study also found that these oligomers released from absorbable PLA plastic could self-aggregate to form nanoplastic particles, which caused acute intestinal inflammation of mice [16]. Given the significant differences between absorbable and nonabsorbable plastics, it is now urgent to investigate the potential toxicity of these released absorbable MPs release from medical plastics.

5. Conclusions

This study focuses on the MPs release from PGA based absorbable sutures and nonabsorbable sutures by soaking in the SBF. Raman tests found that PGA based absorbable sutures released a high number of crystalline MPs while no MPs were released from the nonabsorbable sutures of PP and PA after soaking in the SBF for 8 weeks. A typical PGA 100 suture released 0.63 ± 0.087 million micro (MPs > 1 μm) and 1.96 ± 0.04 million nano (NPs, 200–1000 nm) plastics per centimeter. PGA co-blended with 10–25% L-lactide or epsilon-caprolactone resulted in a two orders of magnitude lower level of MP release. MPs release rate ranking is PGA 100 > > PGA 90 > PGA 75 > > PP = PA. In situ test confirmed that PGA-based suture underwent a typical bulk degradation process, resulting in a bulk disintegration and sharp-edged MPs release. These results underscore the need to assess the release of nano- and microplastics from medical polymers when applied in the human body and to evaluate possible risks to human health.

CRediT authorship contribution statement

Li Dunzhu: Conceptualization, Methodology, Project administration, Supervision, Writing – review & editing. **Wang Jing Jing:** Conceptualization, Methodology, Project administration, Supervision, Writing – review & editing. **Boland John:** Conceptualization, Methodology, Project administration, Supervision, Writing – review & editing. **Xiao Liwen:** Conceptualization, Methodology, Project administration, Supervision, Writing – review & editing. **Shi Yunhong:** Writing – original draft, Formal analysis, Investigation, Methodology. **Hill Christopher:** Investigation, Writing – review & editing. **Yang Luming:** Investigation, Writing – review & editing. **Sheerin Emmet D.:** Investigation, Writing – review & editing. **Pilliadugula Rekha:** Investigation, Writing – review & editing.

Environmental Implication

Nano and microplastics (MPs) are a global concern due to the potential risk to human health and the environment. The typical polyglycolic acid (PGA) based medical polymer-suture underwent a typical bulk degradation process and released 0.63 ± 0.087 million micro (MPs > 1 µm) and 1.96 ± 0.04 million nano (NPs, 200–1000 nm) plastics per centimeter. Furthermore, the degradation monomer (glycolic acid) from PGA-MPs could acidify the surrounding environment. There is an urgent need to assess MPs and NPs release from medical polymers while applied to the human body and the possible risk associated with the discarded medical polymer to the environment.

Declaration of Competing Interest

The authors declare that they have no known competing financial interests or personal relationships that could have appeared to influence the work reported in this paper.

Data Availability

Data will be made available on request.

Acknowledgments

Appendix. Supplementary materials

The Supporting Information associated with this article can be found in another file (4 Figures, 1 Table, 1 Note).

Appendix A. Supporting information

Supplementary data associated with this article can be found in the online version at doi:10.1016/j.jhazmat.2024.133559.

References

[1] Athanasiou, K.A., Niederauer, G.G., Agrawal, C.M., 1996. Sterilization, toxicity, biocompatibility and clinical applications of polylactic acid/polyglycolic acid copolymers. Biomater 17 (2), 93–102.

[2] Bernard, M., Jubeli, E., Pungente, M.D., Yagoubi, N., 2018. Biocompatibility of polymer-based biomaterials and medical devices–regulations, in vitro screening and risk-management. Biomater Sci 6 (8), 2025–2053.

[3] Black, J., 2005. Biological Performance of Materials: Fundamentals of Biocompatibility. CRC Press.

[4] Boccaccini, A.R., Stamboulis, A.G., Rashid, A., Roether, J.A., 2003. Composite surgical sutures with bioactive glass coating. J Biomed Mater Res B Appl Biomater 67 (1), 618–626.

[5] Budak, K., Sogut, O., Sezer, U.A., 2020. A review on synthesis and biomedical applications of polyglycolic acid. J Polym Res 27 (8), 1–19.

[6] Capek, L., Jacquet, E., Dzan, L., Simunek, A., 2012. The analysis of forces needed for the suturing of elliptical skin wounds. Med Biol Eng Comput 50, 193–198.

[7] Cassanas, G., Kister, G., Fabregue, E., Morssli, M., Bardet, L., 1993. Raman spectra of glycolic acid, l-lactic acid and d, l-lactic acid oligomers. Spectrochim Acta Part A: Mol Spectrosc 49 (2), 271–279.

[8] Choi, D., Hwang, J., Bang, J., Han, S., Kim, T., Oh, Y., Hwang, Y., Choi, J., Hong, J., 2021. In vitro toxicity from a physical perspective of polyethylene microplastics based on statistical curvature change analysis. Sci Total Environ 752, 142242.

[9] Cole, M., Webb, H., Lindeque, P.K., Fileman, E.S., Halsband, C., Galloway, T.S., 2014. Isolation of microplastics in biota-rich seawater samples and marine organisms. Sci Rep 4 (1), 1–8.

[10] Cui, Q., Yang, X., Li, J., Miao, Y., Zhang, X., 2022. Microplastics generation behavior of polypropylene films with different crystalline structures under UV irradiation. Polym Degrad Stab 199, 109916.

[11] Dang, F., Wang, Q., Huang, Y., Wang, Y., Xing, B., 2022. Key knowledge gaps for one health approach to mitigate nanoplastic risks. Eco-Environ Health 1 (1), 11–22.

[12] Danopoulos, E., Twiddy, M., West, R., Rotchell, J.M., 2021. A rapid review and meta-regression analyses of the toxicological impacts of microplastic exposure in human cells. J Hazard Mater 127861.

[13] Dennis, C., Sethu, S., Nayak, S., Mohan, L., Morsi, Y., Manivasagam, G., 2016. Suture materials—current and emerging trends. J Biomed Mater Res A 104 (6), 1544–1559.

[14] Eenink, M., Albers, H., Rieke, J., Olijslager, J., Greidanus, P. and Feijen, J. 1985 Biodegradable hollow fibers for the controlled release of drugs, pp. 49–50.

[15] Eerkes-Medrano, D., Thompson, R., 2018. Microplastic Contamination in Aquatic Environments. Elsevier, pp. 95–132.

[16] Fang, M. and Wang, M. 2023. Oligomer nanoparticle release from a biodegradable plastic triggers acute gut inflammation. Nature nanotechnology.

[17] Frazza, E., Schmitt, E., 1971. A new absorbable suture. J Biomed Mater Res 5 (2), 43–58.

[18] Freudenberg, S., Rewerk, S., Kaess, M., Weiss, C., Dorn-Beinecke, A., Post, S., 2004. Biodegradation of absorbable sutures in body fluids and pH buffers. Eur Surg Res 36 (6), 376–385.

[19] Fu, B.X., Hsiao, B.S., Chen, G., Zhou, J., Koyfman, I., Jamiolkowski, D.D., Dormier, E., 2002. Structure and property studies of bioabsorbable poly (glycolide-co-lactide) fiber during processing and in vitro degradation. Polymer 43 (20), 5527–5534.

[20] Galloway, T.S., Cole, M., Lewis, C., 2017. Interactions of microplastic debris throughout the marine ecosystem. Nat Ecol Evol 1 (5), 1–8.

[21] Gigault, J., Hadri, El, Nguyen, H., Grassl, B., Rowenczyk, B., Tufenkji, L., Feng, S, N., M, Wiesner, 2021. Nanoplastics are neither microplastics nor engineered nanoparticles. Nat Nanotechnol 1–7.

[22] González-Pleiter, M., Tamayo-Belda, M., Pulido-Reyes, G., Amariei, G., Leganés, F., Rosal, R., Fernández-Piñas, F., 2019. Secondary nanoplastics released from a biodegradable microplastic severely impact freshwater environments. Environ Sci: Nano 6 (5), 1382–1392.

[23] Grainger, J.R., Konkel, J.E., Zangerle-Murray, T., Shaw, T.N., 2017. Macrophages in gastrointestinal homeostasis and inflammation. Pflüg Arch-Eur J Physiol 469 (3-4), 527–539.

[24] Greenberg, J.A., Clark, R.M., 2009. Advances in suture material for obstetric and gynecologic surgery. Rev Obstet Gynecol 2 (3), 146.

[25] Guo, Z., Yang, C., Zhou, Z., Chen, S., Li, F., 2017. Characterization of biodegradable poly (lactic acid) porous scaffolds prepared using selective enzymatic degradation for tissue engineering. RSC Adv 7 (54), 34063–34070.

[26] Gurappa, I., 2002. Characterization of different materials for corrosion resistance under simulated body fluid conditions. Mater Charact 49 (1), 73–79.

[27] Haude, M., Erbel, R., Erne, P., Verheye, S., Degen, H., Böse, D., Vermeersch, P., Wijnbergen, I., Weissman, N., Prati, F., 2013. Safety and performance of the drug-eluting absorbable metal scaffold (DREAMS) in patients with de-novo coronary lesions: 12 month results of the prospective, multicentre, first-in-man BIOSOLVE-I trial. Lancet 381 (9869), 836–844.

[28] He, Y.-J., Qin, Y., Zhang, T.-L., Zhu, Y.-Y., Wang, Z.-J., Zhou, Z.-S., Xie, T.-Z., Luo, X.-D., 2021. Migration of (non-) intentionally added substances and microplastics from microwavable plastic food containers. J Hazard Mater 417, 126074.

[29] Hernandez, L.M., Xu, E.G., Larsson, H.C., Tahara, R., Maisuria, V.B., Tufenkji, N., 2019. Plastic teabags release billions of microparticles and nanoparticles into tea. Environ Sci Technol 53 (21), 12300–12310.

[30] Hodge, W., Fijan, R., Carlson, K., Burgess, R., Harris, W., Mann, R., 1986. Contact pressures in the human hip joint measured in vivo. Proc Natl Acad Sci 83 (9), 2879–2883.

[31] Hong, Y., Oh, J., Lee, I., Fan, C., Pan, S.-Y., Jang, M., Park, Y.-K., Kim, H., 2021. Total-organic-carbon-based quantitative estimation of microplastics in sewage. J Chem Eng 423, 130182.

[32] Jeon, S., Lee, D.-K., Jeong, J., Yang, S.I., Kim, J.-S., Kim, J., Cho, W.-S., 2021. The reactive oxygen species as pathogenic factors of fragmented microplastics to macrophages. Environ Pollut 281, 117006.

[33] Karami, A., Golieskardi, A., Choo, C.K., Larat, V., Galloway, T.S., Salamatinia, B., 2017. The presence of microplastics in commercial salts from different countries. Sci Rep 7 (1), 1–11.

[34] Kister, G., Cassanas, G., Vert, M., 1997. Morphology of poly (glycolic acid) by IR and Raman spectroscopies. Spectrochim Acta - A: Mol Biomol Spectrosc 53 (9), 1399–1403.

[35] Klompmaker, J., Jansen, H., Veth, R., De Groot, J., Nijenhuis, A., Pennings, A., 1991. Porous polymer implant for repair of meniscal lesions: a preliminary study in dogs. Biomater 12 (9), 810–816.

[36] Kokubo, T., Takadama, H., 2007. Simulated body fluid (SBF) as a standard tool to test the bioactivity of implants. Handb Biominer: Biol Asp Struct Form 97–109.

[37] Kotula, A.P., Snyder, C.R., Migler, K.B., 2017. Determining conformational order and crystallinity in polycaprolactone via Raman spectroscopy. Polymer 117, 1–10.

[38] Li, C., Guo, C., Fitzpatrick, V., Ibrahim, A., Zwierstra, M.J., Hanna, P., Lechtig, A., Nazarian, A., Lin, S.J., Kaplan, D.L., 2020. Design of biodegradable, implantable devices towards clinical translation. Nat Rev Mater 5 (1), 61–81.

[39] Li, D., Sheerin, E.D., Shi, Y., Xiao, L., Yang, L., Boland, J.J., Wang, J.J., 2022. Alcohol pretreatment to eliminate the interference of micro additive particles in the identification of microplastics using Raman spectroscopy. Environ Sci Technol 56 (17), 12158–12168.

[40] Li, D., Yang, L., Kavanagh, R., Xiao, L., Shi, Y., Kehoe, D.K., Sheerin, E.D., Gun'ko, Y.K., Boland, J.J., Wang, J.J., 2021. Sampling, identification and characterization of microplastics release from polypropylene baby feeding bottle during daily use. J Vis Exp, e62545.

[41] Liu, Y., Nelson, T., Chakroff, J., Cromeens, B., Johnson, J., Lannutti, J., Besner, G. E., 2019. Comparison of polyglycolic acid, polycaprolactone, and collagen as scaffolds for the production of tissue engineered intestine. J Biomed Mater 107 (3), 750–760.

[42] Lloyd, B., 2023. Estimating demand for healthcare facilities in rural developing countries. Agric Rural Stud 1 (3), 0018-0018.

[43] Merkley, S.D., Moss, H.C., Goodfellow, S.M., Ling, C.L., Meyer-Hagen, J.L., Weaver, J., Campen, M.J., Castillo, E.F., 2022. Polystyrene microplastics induce an immunometabolic active state in macrophages. Cell Biol Toxicol 38 (1), 31–41.

[44] Min, K., Cuiffi, J.D., Mathers, R.T., 2020. Ranking environmental degradation trends of plastic marine debris based on physical properties and molecular structure. Nat Commun 11 (1), 1–11.

[45] Minoda, Y., Kobayashi, A., Iwaki, H., Miyaguchi, M., Kadoya, Y., Ohashi, H., Yamano, Y., Takaoka, K., 2003. Polyethylene wear particles in synovial fluid after total knee arthroplasty. Clin Orthop Relat Research® 410, 165–172.

[46] Omar, W.A., Kumbhani, D.J., 2019. The current literature on bioabsorbable stents: a review. Curr Atheroscler Rep 21 (12), 1–9.

[47] Pillai, C.K.S., Sharma, C.P., 2010. Absorbable polymeric surgical sutures: chemistry, production, properties, biodegradability, and performance. J Biomater Appl 25 (4), 291–366.

[48] Ramakrishna, S., Mayer, J., Wintermantel, E., Leong, K.W., 2001. Biomedical applications of polymer-composite materials: a review. Compos Sci Technol 61 (9), 1189–1224.

[49] Ramsperger, A., Narayana, V., Gross, W., Mohanraj, J., Thelakkat, M., Greiner, A., Schmalz, H., Kress, H., Laforsch, C., 2020. Environmental exposure enhances the internalization of microplastic particles into cells. Sci Adv 6 (50), eabd1211.

[50] Ramsperger, A.F., Bergamaschi, E., Panizzolo, M., Fenoglio, I., Barbero, F., Peters, R., Undas, A., Purker, S., Giese, B., Lalyer, C.R., 2022. Nano-and microplastics: a comprehensive review on their exposure routes, translocation, and fate in humans. NanoImpact, 100441.

[51] Renardy, M., Planck, H., Dauner, M., 1992. Degradation Phenomena on Polymeric Biomaterials. Springer.

[52] Schymanski, D., Goldbeck, C., Humpf, H.-U., Fürst, P., 2018. Analysis of microplastics in water by micro-Raman spectroscopy: release of plastic particles from different packaging into mineral water. Water Res 129, 154–162.

[53] Schymanski, D., Oßmann, B.E., Benismail, N., Boukerma, K., Dallmann, G., Von der Esch, E., Fischer, D., Fischer, F., Gilliland, D., Glas, K., 2021. Analysis of microplastics in drinking water and other clean water samples with micro-Raman and micro-infrared spectroscopy: minimum requirements and best practice guidelines. Anal Bioanal Chem 1–26.

[54] Shi, Y., Li, D., Xiao, L., Mullarkey, D., Kehoe, D.K., Sheerin, E.D., Barwich, S., Yang, L., Gun'ko, Y.K., Shvets, I.V., Mobius, M.E., Boland, J.J., Wang, J.J., 2022.

[55] Real-world natural passivation phenomena can limit microplastic generation in water. J Chem Eng 428, 132466.

[55] Shi, Y., Li, D., Xiao, L., Sheerin, E.D., Mullarkey, D., Yang, L., Bai, X., Shvets, I.V., Boland, J.J., Wang, J.J., 2021. The influence of drinking water constituents on the level of microplastic release from plastic kettles. J Hazard Mater, 127997.

[56] Song, Y.K., Hong, S.H., Jang, M., Han, G.M., Jung, S.W., Shim, W.J., 2017. Combined effects of UV exposure duration and mechanical abrasion on microplastic fragmentation by polymer type. Environ Sci Technol 51 (8), 4368–4376.

[57] Sun, L., Wanasekara, N., Chalivendra, V., Calvert, P., 2015. Nano-mechanical studies on polyglactin sutures subjected to in vitro hydrolytic and enzymatic degradation. J Nanosci Nanotechnol 15 (1), 93–99.

[58] Taylor, M., Daniels, A., Andriano, K., Heller, J., 1994. Six bioabsorbable polymers: in vitro acute toxicity of accumulated degradation products. J Appl Biomater 5 (2), 151–157.

[59] Taysi, A.E., Ercal, P., Sismanoglu, S., 2021. Comparison between tensile characteristics of various suture materials with two suture techniques: an in vitro study. Clin Oral Investig 25, 6393–6401.

[60] Tokiwa, Y., Calabia, B.P., Ugwu, C.U., Aiba, S., 2009. Biodegradability of plastics. Int J Mol Sci 10 (9), 3722–3742.

[61] Tranquillo, E., Barrino, F., Dal Poggetto, G., Blanco, I., 2019. Sol–gel synthesis of silica-based materials with different percentages of PEG or PCL and high chlorogenic acid content. Materials 12 (1), 155.

[62] Vethaak, A.D., Legler, J., 2021. Microplastics and human health. Science 371 (6530), 672–674.

[63] Visscher, G., Robison, R., Maulding, H., Fong, J., Pearson, J., Argentieri, G., 1986. Biodegradation of and tissue reaction to poly (DL-lactide) microcapsules. J Biomed Mater Res 20 (5), 667–676.

[64] Von Burkersroda, F., Schedl, L., Göpferich, A., 2002. Why degradable polymers undergo surface erosion or bulk erosion. Biomater 23 (21), 4221–4231.

[65] Wei, X.-F., Bohlén, M., Lindblad, C., Hedenqvist, M., Hakonen, A., 2021. Microplastics generated from a biodegradable plastic in freshwater and seawater. Water Res 198, 117123.

[66] Wesełucha-Birczyńska, A., Świętek, M., Sołtysiak, E., Galiński, P., Piekara, K., Błażewicz, M., 2015. Raman spectroscopy and the material study of nanocomposite membranes from poly (ε-caprolactone) with biocompatibility testing in osteoblast-like cells. Analyst 140 (7), 2311–2320.

[67] Winkler, A., Santo, N., Ortenzi, M.A., Bolzoni, E., Bacchetta, R., Tremolada, P., 2019. Does mechanical stress cause microplastic release from plastic water bottles? Water Res 166, 115082.

[68] Wolff, C.M., Singer, D., Schmidt, A., Bekeschus, S., 2023. Immune and inflammatory responses of human macrophages, dendritic cells, and T-cells in presence of micro-and nanoplastic of different types and sizes. J Hazard Mater 459, 132194.

[69] Woodall, L.C., Sanchez-Vidal, A., Canals, M., Paterson, G.L., Coppock, R., Sleight, V., Calafat, A., Rogers, A.D., Narayanaswamy, B.E., Thompson, R.C., 2014. The deep sea is a major sink for microplastic debris. R Soc Open Sci 1 (4), 140317.

[70] Woodard, L.N., Grunlan, M.A., 2018. Hydrolytic degradation and erosion of polyester biomaterials. ACS Macro Lett.

[71] Wu, H., Guo, T., Zhou, F., Bu, J., Yang, S., Dai, Z., Teng, C., Ouyang, H., Wei, W., 2022. Surface coating prolongs the degradation and maintains the mechanical strength of surgical suture in vivo. Colloids Surf B: Biointerfaces 209, 112214.

[72] Yancey, P.H., Gerringer, M.E., Drazen, J.C., Rowden, A.A., Jamieson, A., 2014. Marine fish may be biochemically constrained from inhabiting the deepest ocean depths. Proc Natl Acad Sci 111 (12), 4461–4465.

[73] Yilmaz, B., Pazarceviren, A.E., Tezcaner, A., Evis, Z., 2020. Historical development of simulated body fluids used in biomedical applications: a review. Microchem J 155, 104713.